Thesis
N42

Library
U. S. Naval Postgraduate School
Annapolis, Md.

TESTING A TURBO-JET COMBUSTION CHAMBER TO CHECK ANALYTICAL DESIGN

A Thesis

Submitted to the Graduate Faculty

of the

University of Minnesota

by

Robert G. Nester

In Partial Fulfillment of the Requirements for

The Degree of

Master of Science in Aeronautical Engineering

ACKNOWLEDGEMENTS

The author would like to express his appreciation to the following people who aided in this investigation: Professor S. J. Robertson and Thomas S. Murphy for their assistance, technical advice, and counseling.

Messrs. K. E. Reimeier, F. Alden, L. Jlausen and C. O. Lund for their assistance in manufacturing and setting up the test equipment.

11471

TABLE OF CONTENTS

	PAGE
SUMMARY	1
INTRODUCTION	1a
PURPOSE OF INVESTIGATION	3
APPARATUS AND INSTRUMENTATION	4
Combustor	4
Test Setup	6
Instrumentation	6
PROCEDURE	9
RESULTS AND DISCUSSION	11
BIBLIOGRAPHY	33
APPENDIX	34
Symbols	36

INDEX TO CHAPTERS

Introduction 1
Early Settlers 5
Early Industries 9
Early Transportation 15
Early Schools 19
Early Churches 23
Early Social Life 27
Early Amusements 31
Early Medicine 35
Early Agriculture 39
Early Commerce 43
Early Banking 47
Early Manufacturing 51
Early Mining 55
Early Lumbering 59
Early Fishing 63
Early Hunting 67
Early Trapping 71
Early Exploration 75
Early Surveying 79
Early Mapping 83
Early Navigation 87
Early Aviation 91
Early Radio 95
Early Television 99
Early Telephone 103
Early Telegraph 107
Early Postal Service 111
Early Newspapers 115
Early Magazines 119
Early Books 123
Early Libraries 127
Early Museums 131
Early Art 135
Early Music 139
Early Literature 143
Early Drama 147
Early Dance 151
Early Sports 155
Early Games 159
Early Toys 163
Early Clothing 167
Early Jewelry 171
Early Cosmetics 175
Early Hairstyles 179
Early Footwear 183
Early Headwear 187
Early Eyewear 191
Early Gloves 195
Early Handbags 199
Early Umbrellas 203
Early Canes 207
Early Watches 211
Early Clocks 215
Early Calendars 219
Early Weights and Measures 223
Early Money 227
Early Coins 231
Early Stamps 235
Early Flags 239
Early Seals 243
Early Coats of Arms 247
Early Mottoes 251
Early Songs 255
Early Poems 259
Early Prayers 263
Early Sermons 267
Early Hymns 271
Early Funerals 275
Early Weddings 279
Early Births 283
Early Deaths 287
Early Cemeteries 291
Early Epitaphs 295
Early Ghosts 299
Early Witches 303
Early Devils 307
Early Angels 311
Early Saints 315
Early Sinners 319
Early Heaven 323
Early Hell 327
Early Purgatory 331
Early Limbo 335
Early Nirvana 339
Early Reincarnation 343
Early Transmigration 347
Early Metempsychosis 351
Early Pantheism 355
Early Polytheism 359
Early Monotheism 363
Early Atheism 367
Early Agnosticism 371
Early Humanism 375
Early Rationalism 379
Early Empiricism 383
Early Idealism 387
Early Realism 391
Early Nominalism 395
Early Conceptualism 399
Early Skepticism 403
Early Stoicism 407
Early Epicureanism 411
Early Cynicism 415
Early Hedonism 419
Early Utilitarianism 423
Early Pragmatism 427
Early Existentialism 431
Early Phenomenology 435
Early Structuralism 439
Early Post-Structuralism 443
Early Deconstruction 447
Early Post-Modernism 451
Early Post-Colonialism 455
Early Feminism 459
Early Gender Studies 463
Early Queer Theory 467
Early Critical Theory 471
Early Cultural Studies 475
Early Media Studies 479
Early Communication Studies 483
Early Information Theory 487
Early Cybernetics 491
Early Systems Theory 495
Early Chaos Theory 499
Early Complexity Theory 503
Early Network Theory 507
Early Graph Theory 511
Early Game Theory 515
Early Decision Theory 519
Early Probability Theory 523
Early Statistics 527
Early Data Analysis 531
Early Machine Learning 535
Early Artificial Intelligence 539
Early Robotics 543
Early Automation 547
Early Computing 551
Early Internet 555
Early World Wide Web 559
Early Social Media 563
Early Blogging 567
Early Podcasting 571
Early Vlogging 575
Early Streaming 579
Early Gaming 583
Early Esports 587
Early Virtual Reality 591
Early Augmented Reality 595
Early Mixed Reality 599
Early Extended Reality 603
Early Metaverse 607
Early Blockchain 611
Early Cryptocurrency 615
Early NFTs 619
Early Web3 623
Early Decentralization 627
Early Tokenization 631
Early Smart Contracts 635
Early Oracles 639
Early Interoperability 643
Early Scalability 647
Early Sustainability 651
Early Regulation 655
Early Governance 659
Early Ethics 663
Early Morality 667
Early Law 671
Early Justice 675
Early Rights 679
Early Freedom 683
Early Equality 687
Early Democracy 691
Early Republic 695
Early Monarchy 699
Early Empire 703
Early Colonialism 707
Early Imperialism 711
Early Nationalism 715
Early Patriotism 719
Early Militarism 723
Early Pacifism 727
Early Peace 731
Early War 735
Early Revolution 739
Early Reform 743
Early Progress 747
Early Decline 751
Early Fall 755
Early Rise 759
Early Cycles 763
Early Seasons 767
Early Weather 771
Early Climate 775
Early Geography 779
Early Geology 783
Early Paleontology 787
Early Archaeology 791
Early Anthropology 795
Early Sociology 799
Early Psychology 803
Early Neuroscience 807
Early Biology 811
Early Chemistry 815
Early Physics 819
Early Astronomy 823
Early Cosmology 827
Early Mathematics 831
Early Logic 835
Early Philosophy 839
Early Theology 843
Early Religion 847
Early Spirituality 851
Early Mysticism 855
Early Occultism 859
Early Esotericism 863
Early Hermeticism 867
Early Alchemy 871
Early Astrology 875
Early Numerology 879
Early Tarot 883
Early Divination 887
Early Magic 891
Early Miracles 895
Early Prophecy 899
Early Apocalypse 903
Early Eschatology 907
Early Conclusion 911

SUMMARY

The results obtained in this investigation to establish the validity of certain pressure drop parameters used in the design of a turbo-jet combustion chamber indicate the performance of the combustor can be predicted by analytical methods.

All computed values of both the friction pressure drop and the pressure drop due to momentum changes with heat addition were lower, in that region of air flows wherein the combustor would normally operate, than those indicated by analysis of the experimental data. The maximum observed error of eight percent occurred for the condition of 4.5 pounds per second air flow. The average percentage error over the entire operating range investigated was approximately 2 percent. The combustor inlet air conditions, under which these runs were made was equivalent to a simulated altitude of 27,000 feet at the design point investigated.

The reproducibility of experimental data was difficult. Allowance must be made for obstructions or irregularities of the flow passages as warping of the combustor basket, or carbon depositions. In the final analysis, for accurately computing the total pressure drop across the combustor, the effect of mixing the relatively cold secondary air with the products of combustion must be taken into account.

CONCLUSION

INTRODUCTION

All turbo-jet engines add energy to air taken in from the surrounding atmosphere and exhaust the products at a higher velocity thus producing thrust. At present the most common method of adding the energy necessary is through the combustion of hydrocarbon fuels with air in the combustion chamber.

The flow of gas through a combustion chamber is accompanied by losses that effect the overall efficiency of the turbo-jet engine to a marked degree. The losses in the combustion chamber may be classified as the total friction pressure loss due to configuration and friction and the pressure loss due to the momentum change with heat addition. Friction pressure losses result from the turbulent flow of the gases over the metal surfaces of the ducting and through the orifices leading into the combustion zone. These losses can be measured during non-firing runs with the combustion chamber, and their values used in computing the pressure loss due to momentum changes during firing runs. This is an approximation but the percentage error is very small. Actually there is a change in the density of the entering air due to a change in temperature that is not indicated in a non-firing run.

Friction pressure losses are usually responsible for two-thirds of the total pressure loss, and is highest in contra-flow combustion chambers and lowest in straight flow chambers with low entrance velocities.

The momentum pressure losses occur as a result of the combustion process in changing the velocity and density of the gases. An exact solution for the momentum pressure loss in a duct of constant cross-sectional area is presented in the appendix. Normally an exact solution is not required when the Mach numbers in the combustion zone are on the order of 0.2 or less than 0.3. The exact solution presented is modified to the extent that the addition of fuel and area change has been neglected. Therefore, the calculated momentum pressure loss will be lower than that derived by experiment.

The importance of minimizing the total pressure loss in the combustor is comparable with keeping the efficiencies of the compressor and turbine as high as possible. Combustion chambers must be designed for the lowest possible pressure drop due to friction and this is possible by eliminating abrupt changes in section, reverse turns in the ducting, minimum initial velocity in the flow passages and maximum area flow passages.

PURPOSE OF INVESTIGATION

It is the purpose of this investigation to establish the validity of certain analytical pressure loss design parameters used in the design of a turbo-jet combustion chamber of similar configuration. The check will be made by comparison with experimental data. In the case of the friction pressure drop, a second comparison will be made using the method set forth in the National Advisory Committee for Aeronautics, Technical Note, Number 1180.

As more and more information of this sort is accumulated the design of combustion chambers for turbo-jet engines will become less of a cut and try process and the need for expensive experimental test setups will be lessened.

APPARATUS AND INSTRUMENTATION

Combustor

The combustor used in these tests was one of fourteen used in the General Motors J-33 Turbo-Jet Engine. It was a special combustor, modified to the extent that the inner-combustor connecting flame tubes were not included in its construction. A sketch of the combustor is shown in Figure 2.

A special air adapter was made to fit the outer liner to eliminate certain variances in the entering air flow. The air adapter provides the mounting for the fuel nozzle, the igniter plug, and the inner liner dome and also supports the forward end of the outer combustion chamber. The inner liner is supported at the entrance end by the dome, and is positioned at the exit ends by a liner-locating dowel. The groves at the forward end of the outer combustion chamber retain two piston rings. These rings enter into the counter-bore of the adapter, forming an air seal between the adapter and the outer combustion chamber, and provides for any expansion or contraction.

Air enters the outer and inner combustion chambers through the adapter. Primary air is introduced into the combustion zone through a series of holes surrounding the

fuel nozzle in the center of the flame tube dome and through holes in the upstream section of the inner combustion chamber. The air entering the holes around the fuel nozzle is deflected by spiral plates inside the dome. This allows maximum mixing of the fuel with the incoming air while establishing a low velocity ignition area with some control of the flame front.

Secondary air, necessary for completion of combustion and cooling, is introduced through a series of 5/8 inch holes and louvres located in the inner combustion chamber downstream from the primary air entry.

The fuel injection system for the combustor consists of an electrically driven fuel pump and one fuel nozzle of the hollow cone spray type. In the nozzle, fuel flows in through tangetial slots in the spray tip and out through the tip orifice into the combustion chamber. At fuel pressures below 125 pounds per square inch the arc of the spray is approximately seventy degrees. At higher pressures the arc narrows and the flow is extended farther into the combustion chamber.

The fuel ignition system employed is that of a high intensity spark combined with an acetylene gas jet. The acetylene gas is fed into the cooling air space between the electrodes and the surrounding ceramic insulation. This insures a positive initial burning and eliminates explosive hot starts. The spark plug used was a General Electric Model 7 HS 40A2.

Test Setup

The general arrangement of the test setup is diagrammatically shown in Figure 1. Air was supplied by the auxiliary compressor section of a 1710 Allison Vee 12 engine. (Figure 5) Desired bomsutor inlet air conditions were obtained by regulation of the Allison engine speed and the combustor exhaust waste gate. The air mass flow was measured by a thin plate orifice located upstream of the compressor.

The inlet duct was fabricated of mild steel to fit the dimensions of the existing air supply ducting and the combustor. The exhaust duct was fabricated of 22 gauge stainless steel and designed to fit the exit of the combustor and to exhaust into the atmosphere. Figure 1 shows the longitudinal cross-section of the inlet duct, the combustor, and the exhaust duct with the location of the instrument stations. Figure 4 shows arrangement of the test setup as installed in the test cell.

Instrumentation

Positions and arrangements of the thermocouples and pressure taps as located in the inlet and exhaust ducts and the combustor are shown diagrammatically in Figure 3.

The velocity profile and the mean velocity of the air flow entering the combustor were determined by three

The general correctness of the head seems to me unquestionably shown in Figure 2c. It is not modified by the distinctly subjective judgment of a JANE AUSTEN (Figure 3) produced however under circumstances favourable to objectivity as the original medium might not flow completely against me. The eye seems flat as represented by a little glossy depilitus covering of the conjunctiva.

The lower part was fortunately of more value to me in the beginning of the modelling and mostly resting upon the construction. The general shape was indicated in the jawbone through the cheek and beginning to fill the back of the mouth could be removed into the shape. Figure 3 shows the longitudinal cross-section of the right head, the construction, and the skeleton that held the skeleton of the lineament plastic. Figure 4 shows comparison of the head before the insertion in the final wall.

Conclusion

Portraits and investigations of the characteristics and drawings have to depend on the kinds and methods there are numerous or the close difficulties in figure 3.

The materials inside the head were helpful of the new film modeling the skeleton many impressions by steps

total head tubes and one static pressure tap located upstream at station 1. This section has a cross-sectional area of .1965 square feet. The temperature of the entering air was measured with an iron-constantan thermocouple.

Determination of the pressure level and the mass flow change of the secondary air along the longitudinal axis of the combustor between the inner and outer liners was attempted through a series of static pressure taps and total head tubes at stations 2, 3, and 4. Station 2 is located just downstream of the primary air inlets at the beginning of the secondary air ports. Stations 3 and 4 are located at the mid-point and at the end of the secondary air ports, respectively. For measuring velocity distribution at the exit of the flame tube during non-firing runs, three pitot-static tubes were inserted into the stream at station 5. For measurement of velocity and total pressure during hot runs, a shielded total head tube and a static pressure tap were used.

Chromel-Alumel thermocouples were used throughout for total temperature measurement of the hot gases, and indications were taken as true with no corrections for radiation or stagnation effects. The temperature distribution of the exhaust gases was measured by a total temperature rake consisting of four thermocouples as shown in Figure 3. The mean combustor exhaust temperature was taken as the arithmetic mean of the temperatures measured

by these four probes.

Mercury manometers were used throughout for total and static pressure measurements. For measuring dynamic pressure level, a bank of six inclined tube mercury manometers was used. Figure 6 shows the instrument recording panel.

Fuel flows were measured with a Fischer and Porter Company Flowrater with Stabil-Vis Viscosity Immune Float.

PROCEDURE

Tests were made to evaluate the performance of the combustion chamber at various pressures and air flows. With the equipment available, the range was limited to a maximum of 46 inches of mercury absolute static pressure at the entrance to the combustion chamber and to three pounds per second air flow.

In order to evaluate the air flow and velocity distribution axially through the combustion chamber, a series of non-firing runs was made at varying combustor inlet static pressures. The data recorded were the total, dynamic, and static pressure level at the entrance; static pressure level of the air stream in the annular space surrounding the inner combustion chamber at the beginning, mid-point, and the end of the secondary air entrances to the combustion zone; and the total and static pressure levels at the exit of the combustor; and the friction pressure drop across the combustor.

To determine the total pressure drop, hot runs were made at set static pressure levels at the combustor entrance with varying mass flows. These runs were made at constant exit temperatures. Total entrance pressure, total and static exit pressures, total entrance temperature, mass

flow and total pressure drop were recorded.

For determining the effect of entrance static pressure on mean temperature rise through the combustor, runs were made at several constant entrance pressures with varying fuel-air ratios. Those data recorded were: entrance temperature, exit temperature, air flow, fuel flow, and total pressure drop.

RESULTS AND DISCUSSION

The data obtained in this investigation to evaluate the performance of the combustor are summarized in Tables 1-5. Those runs wherein blowout or unstable combustion occurred are omitted because they have no bearing in this evaluation. The mean combustor outlet temperature indicated in Table 1 is the arithmetical mean of four readings taken at Station 5. Measured temperatures were very erratic. A representative distribution of combustor exit temperatures may be seen in Figure 8.

The combustor operated at efficiencies above 80 percent and was capable of producing outlet temperatures in excess of that deemed safe for operation at high back pressures. Figure 9 shows the effect of varying the combustor inlet pressure on the efficiency of the combustor. Curves of 100, 80, and 60 percent theoretical temperature rise are included for combustion efficiency estimation. When the entrance pressure was high the combustor operated at efficiencies above 90 percent except at fuel-air ratios of less than 0.01. This is due, in part, to poor atomization of the fuel used in the nozzle at low fuel pressures. The maximum efficiency occurred at an overall fuel-air ratio much leaner than the overall stoichiometric mixture.

As the inlet pressure was increased this maximum remained fairly constant at a fuel-air ratio of 0.014.

The effect of varying the inlet static pressure on total pressure drop is shown graphically in Figure 10. It is seen, that for any one selected air flow, the pressure drop decreased as the inlet pressure was increased. The pressure drop is a function of the inlet velocity which in turn is a function of the density of the gas stream. As the inlet pressure was increased the density of the entering air mass was increased and the velocity necessary to pass the mass flow was decreased. The control of the inlet pressure was made by regulation of the Allison compressor speed and by applying the necessary back pressure by reducing the effective area of the exhaust. Three runs were made at varying inlet pressure to give an indication of the manner in which the pressure drop varied. All runs were made at a mean combustor exit temperature of 1600 degrees Rankine.

Figures 11, 12, and 13 show the comparison of experimental and computed combustion chamber pressure losses. The calculated friction pressure loss by Method I and indicated in Figure 11, is that presented by the National Advisory Committee for Aeronautics, Technical Note Number 1100. This method is based on the assumption that the pressure loss characteristics of the actual combustion chamber can be matched by those of an equivalent combustion chamber of constant cross-sectional area. It is also

assumed that the friction pressure loss takes place before the combustion process. This method was included in this investigation for a comparison check only. The calculated friction pressure drop, indicated Method II in Figure 12, is that presented by J. B. Verdin in a paper on the design of a turbo-jet combustion chamber, and is included in the Appendix.

Figure 13 is a comparison of the experimental momentum pressure drop with that computed. This method of computing the pressure drop due to momentum changes is included in the Appendix. The difference indicated in the curves is largely due to the neglect of the slight area change in the combustor (less than 3 percent) and the effect of the change in momentum involved in the mixing of the hot and cold gas streams.

The altitude condition simulated in this investigation was 27,000 feet density altitude. This simulated altitude prevailed at the design condition of 2.5 pounds per second air flow. The simulated altitude at the combustor entrance was computed from assumed data for a turbo-jet engine having a compressor compression ratio of four and a compressor efficiency of 90 percent.

It was found that the accurate reproduction of data was difficult at low compressor speeds. The Allison engine compressor used in supplying the air has an engine-compressor speed ratio of 8.5 to 1. A surge of 100 rpm engine speed,

therefore, would give an increase or decrease of 350 rpm of the compressor. In an attempt to smooth out the flow of air and approach the steady flow conditions necessary, one bank of the Allison engine was made inoperable. This improved conditions at low mass flows. It is suggested that in future investigations of this type a system of bleed-off be installed to eliminate this condition. At high compressor speeds no serious difficulty was encountered in reproducing data.

TABLE NUMBER 1

EXPERIMENTAL								THEORETICAL		
W_a "Hg	W_f #/HR	W_a #/sec	W_f #/sec	F/A	T_1 °F	T_5 °F	ΔT	100% ΔT	80% ΔT	60% ΔT
.65	53	1.705	0.0147	0.0086	140	525	385	646	518.5	389
.65	62	1.705	0.0172	0.0101	140	652	512			
.65	71	1.705	0.0197	0.01158	140	780	680	862	689	517
.65	79	1.705	0.0219	0.01285	140	916	775			
.65	88	1.705	0.0244	0.0143	140	1040	900			
.65	100	1.705	0.0278	0.0163	140	1176	1035	1210	977	726
.60	110	1.640	0.0306	0.01876	140	1310	1170			
.55	120	1.570	0.0334	0.02125	140	1460	1310	1560	1250	937

ENERGENE DIESEL FUEL # 2

HHV 19600 BTU/LB

SP.GR 0.855

P_a = 29.12 "Hg , T_a = 90°F

P_1 = 34.2 "Hg ABS.

TABLE NUMBER 2

ENTRANCE PRESSURE 37.2 "Hg Abs.							
ω_a "Hg	ω_f #/HR	ω_a #/sec	ω_f #/sec	F/A	T_1 °F	T_5 °F	ΔT
1.1	68	2.22	0.0189	0.0085	160	651	491
1.0	75	2.11	0.0208	0.00985	160	780	620
0.95	82	2.06	0.0228	0.01106	160	915	755
0.86	88	1.96	0.0244	0.01245	160	1040	880
0.84	95	1.937	0.0264	0.01362	160	1175	1015
0.75	106	1.83	0.0294	0.01605	160	1310	1150
0.62	118	1.66	0.0328	0.01975	160	1450	1290
P_a = 29.20 "Hg T_a = 90 °F							

TABLE NUMBER 3

ENTRANCE PRESSURE 43.2 "Hg ABS.							
ω_a "Hg	ω_f #/HR	ω_a #/SEC	ω_f #/SEC	F/A	T_1 °F	T_6 °F	
1.55	72	2.63	0.0200	0.0076	180	631	471
1.4	83	2.50	0.02308	0.00921	180	780	600
1.3	92	2.41	0.0256	0.0106	180	915	735
1.2	100	2.31	0.0278	0.0120	180	1040	860
1.07	110	2.182	0.0305	0.0140	180	1175	995
0.92	119	2.05	0.033	0.0161	180	1310	1130
0.86	128	1.96	0.0355	0.0181	180	1450	1270

P_a = 29.20 "Hg T_a = 90 °F

TABLE NUMBER 4

P_1 "Hg Abs	T_1 °F	W_a "Hg	W_a #/SEC	ΔP_F "Hg MEASURED	$\Delta P/P_1$ MEASURED	ΔP_F #/□ CALCULATED METHOD I	$\Delta P_F/P_1$ METHOD I	ΔP_F METHOD II	$\Delta P_F/P_1$ METHOD II
31.8	120	.35	1.26	0.6	0.0189	48.1	0.022	.75	.0236
33.7	140	.51	1.51	1.1	0.0326	70.6	0.0296	1.1	.0326
35.4	160	.70	1.77	1.4	0.0396	96.5	0.0381	1.49	.0420
39.3	180	1.15	2.281	2.1	0.0534	148	0.0533	2.32	.0590
42.4	205	1.4	2.50	2.8	0.066	171	0.0570	2.69	.0635
45.2	240	1.7	2.75	3.5	0.0774	203.6	0.0636	3.22	.0710

P_a = 29.1 "Hg Abs T_a = 95 °F

TABLE NUMBER 5

(1)											(12)		(14)		(16)	(17)				
P_{T_1} "Hg Abs	W_a #/sec	T_{T_1} °R	ρ #/Ft³	V_1 Ft/sec	q_5 "Hg	P_5 "Hg Abs	M_5	a_5 Ft/sec	V_5 Ft/sec	V_8' Ft/sec	V_1/V_5'	T_{T_8}/T_{T_1}	$(T_{T_8}/T_{T_1})^{\gamma/\gamma-1}$	(T_5/T_1)	$(T_5/T_1)^{\gamma/\gamma-1}$	(12)x(14) / (16)	(17)x(1)	ΔP_H	$\Delta P_H/P_1$	M_B
31.9	1.25	580	0.0761	83.5	1.6	29.4	.28	1986	555	237	.352	2.82	89.5	2.83	31.8	.989	31.585	.315	.0099	.1106
33.8	1.51	600	0.0780	98.5	2.6	29.5	.369	1986	732	306	.340	2.72	76.1	2.661	26.2	.987	33.364	.436	.013	.164
36.6	1.77	620	0.0794	113.4	3.4	29.9	.419	1985	830	341	.3312	2.686	66.9	2.528	22.2	.9845	37.969	.531	.015	.172
39.7	2.281	640	0.0852	136.5	5.8	30.7	.54	1985	1070	440	.310	2.66	40.6	2.160	12.83	.979	38.634	.766	.0196	.222
42.5	2.50	665	0.0886	143.9	7.4	31.4	.602	1985	1230	504	.2854	2.46	390	2.11	11.12	.9785	41.653	.847	.02	.253
46.3	2.70	700	0.0900	155.5	9.5	32.0	.676	1985	1340	550	.2825	2.335	36 8	2.06	10.60	.976	44296	.9046	.02	.277

$P_a = 29.2$ "Hg Abs $T_a = 90°F$ $T_{T_5} = 1635°R$ $\gamma = 1.3$

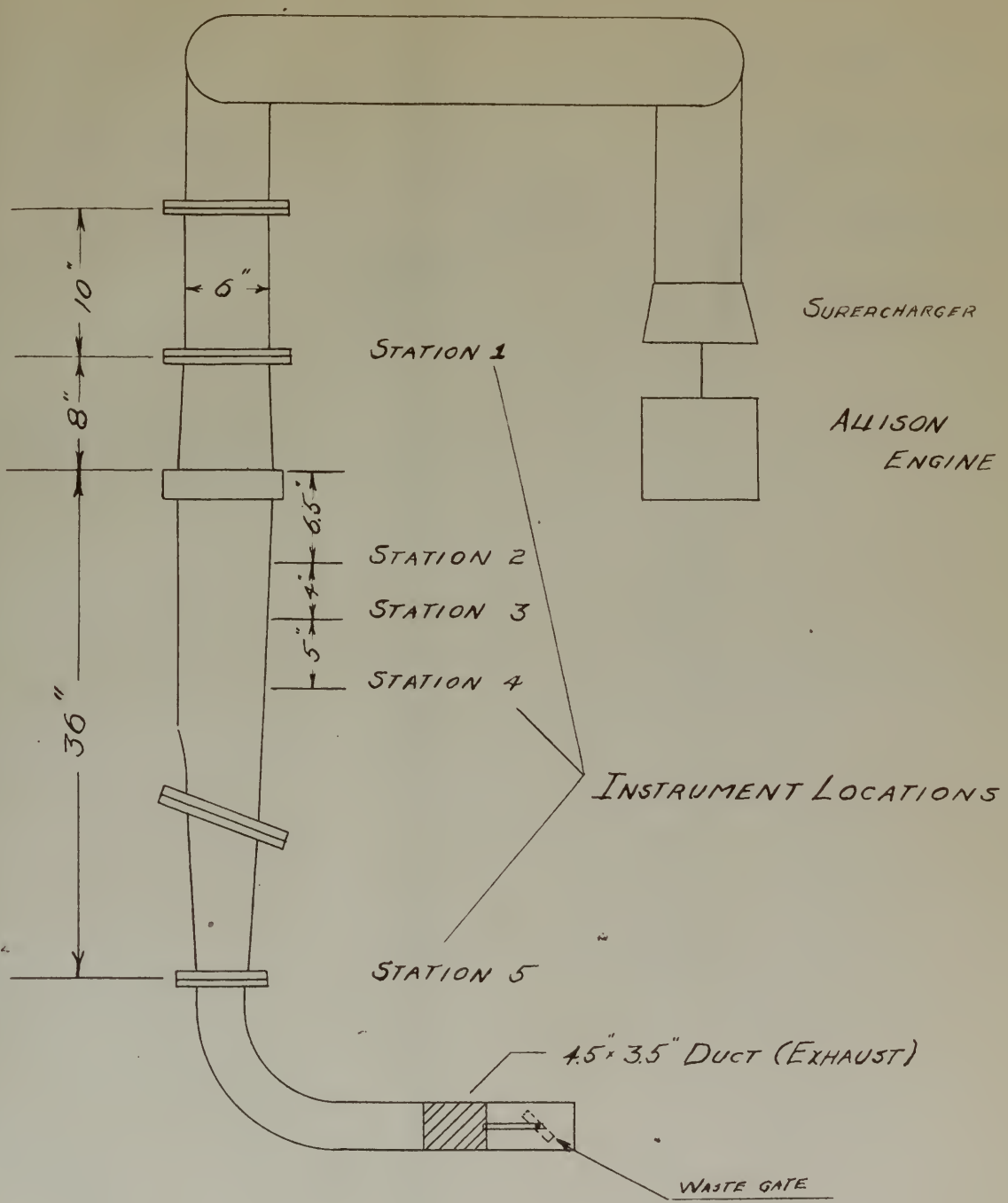
10"
6"
8"
6.5"
4"
5"
36"
SURERCHARGER
ALLISON
ENGINE
STATION 1
STATION 2
STATION 3
STATION 4
INSTRUMENT LOCATIONS
STATION 5
4.5" x 3.5" DUCT (EXHAUST)
WASTE GATE

FIGURE 1

RGN

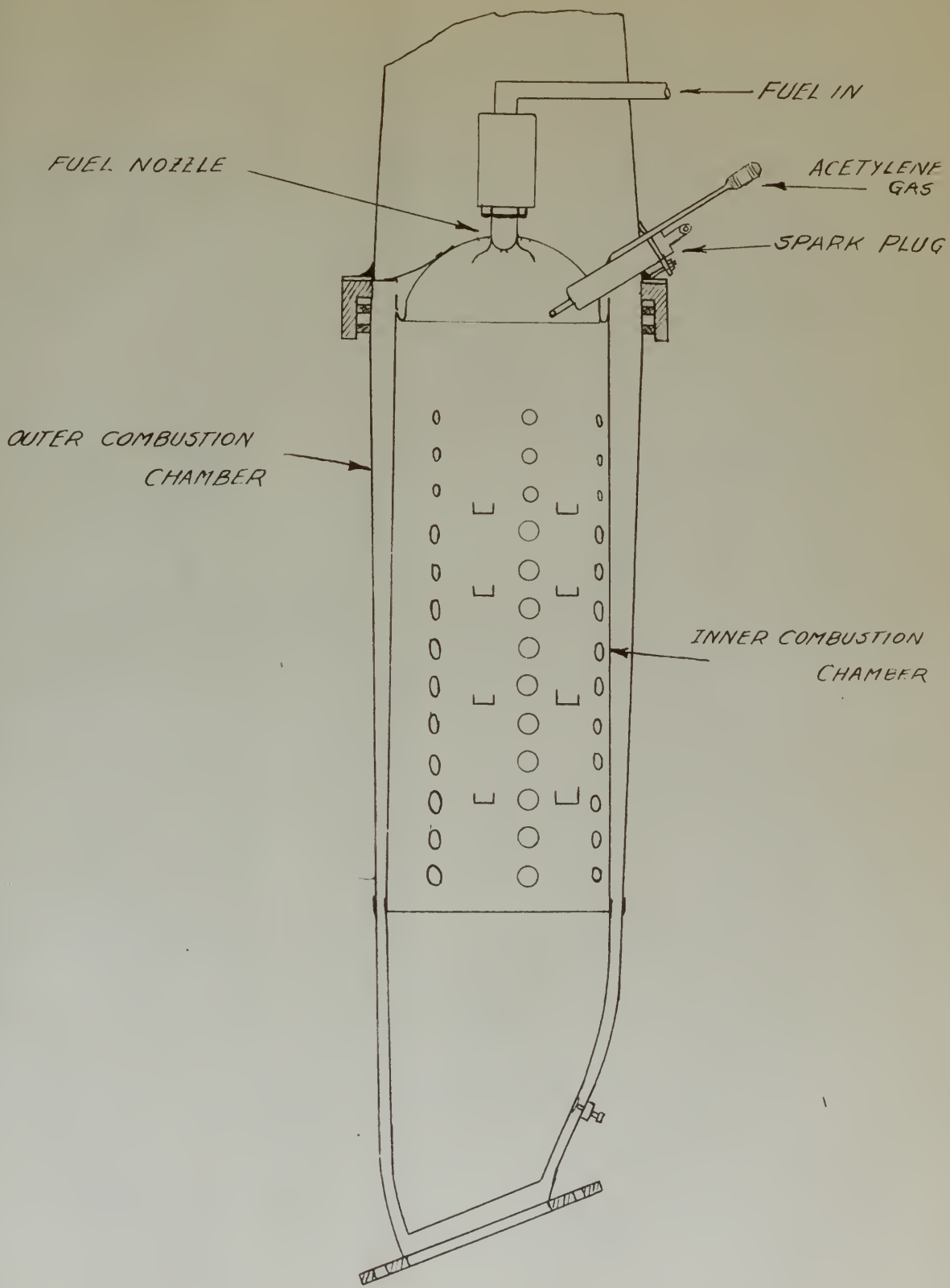
FUEL IN
FUEL NOZZLE
ACETYLENE GAS
SPARK PLUG
OUTER COMBUSTION CHAMBER
INNER COMBUSTION CHAMBER

FIGURE 2

RGN

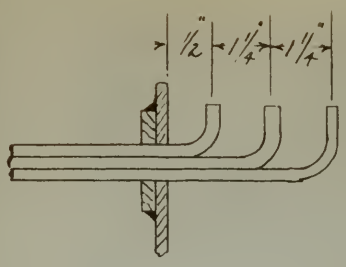

TOTAL HEAD RAKE

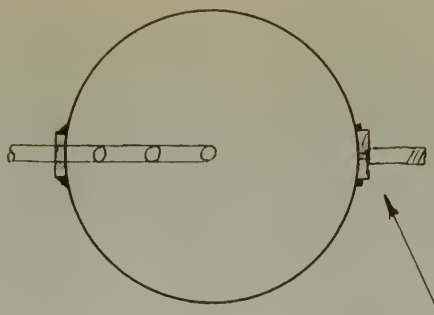

STATIC PRESSURE TAP

STATION 1

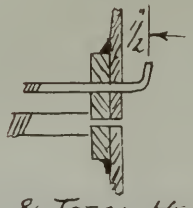

STATIC & TOTAL HEAD TAP

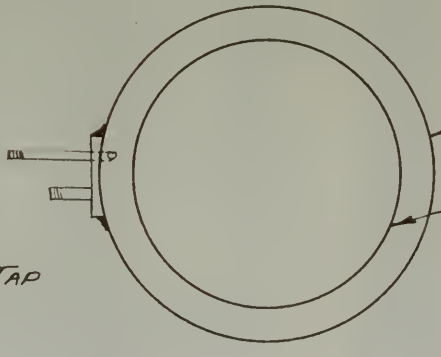

OUTER LINER

INNER LINER

STATION 2, 3, 4.

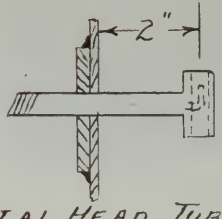

TOTAL HEAD TUBE

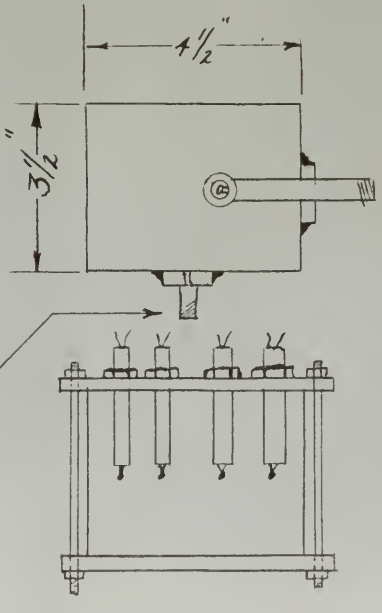

STATIC PRESSURE TAP

STATION 5

C. A. THERMOCOUPLE RAKE

FIGURE 3

RGN

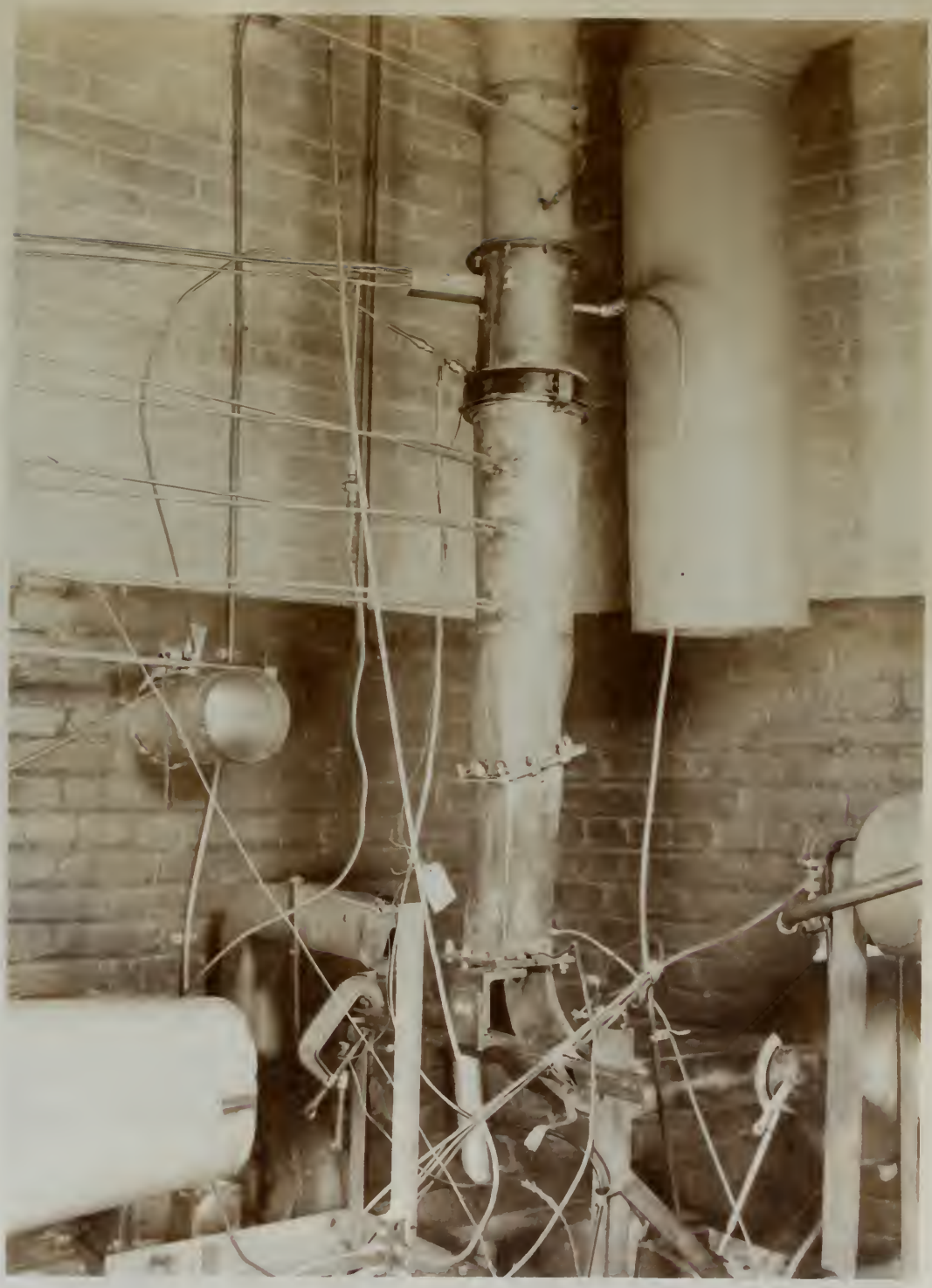

FIGURE 4

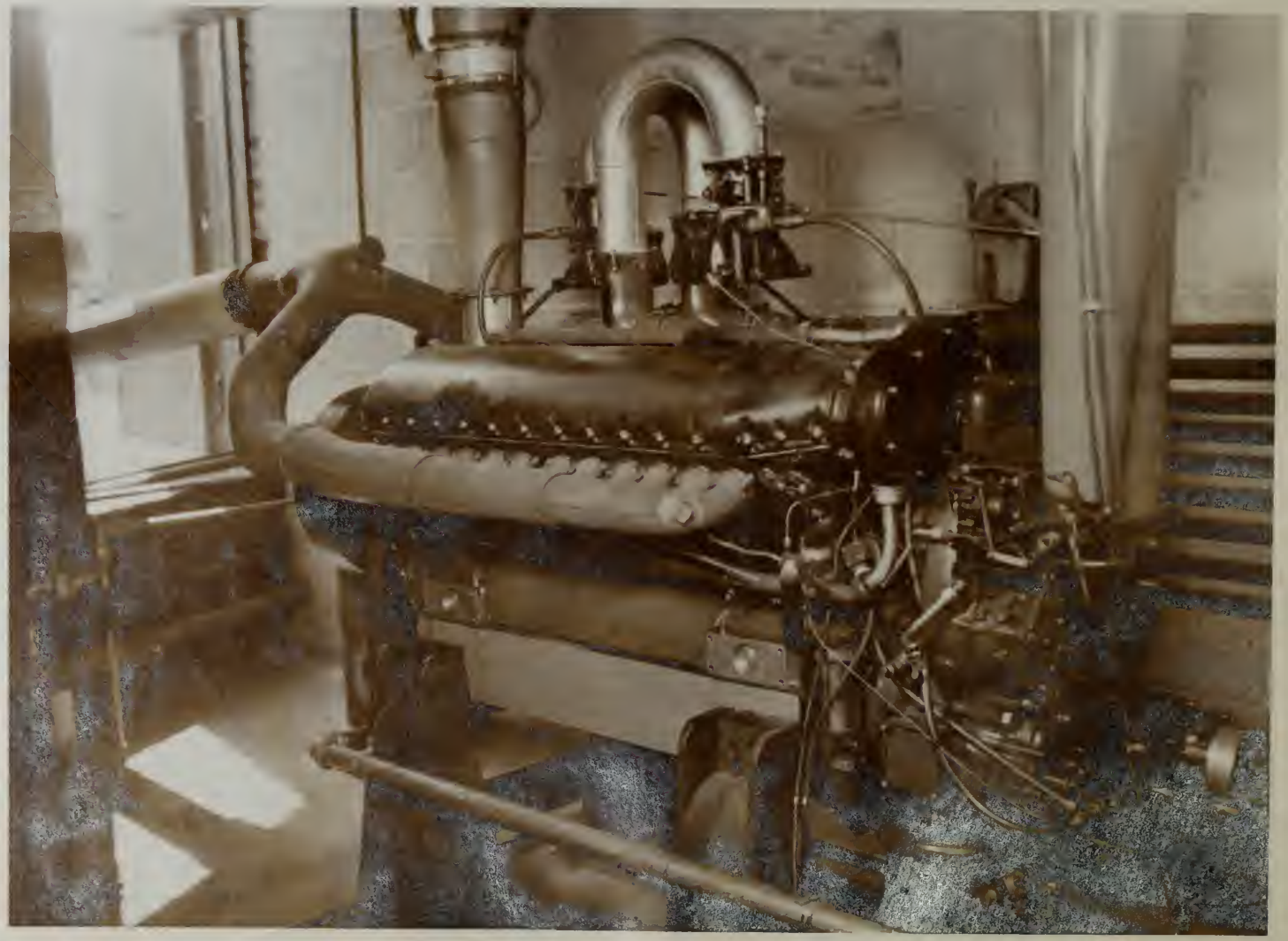

FIGURE 5

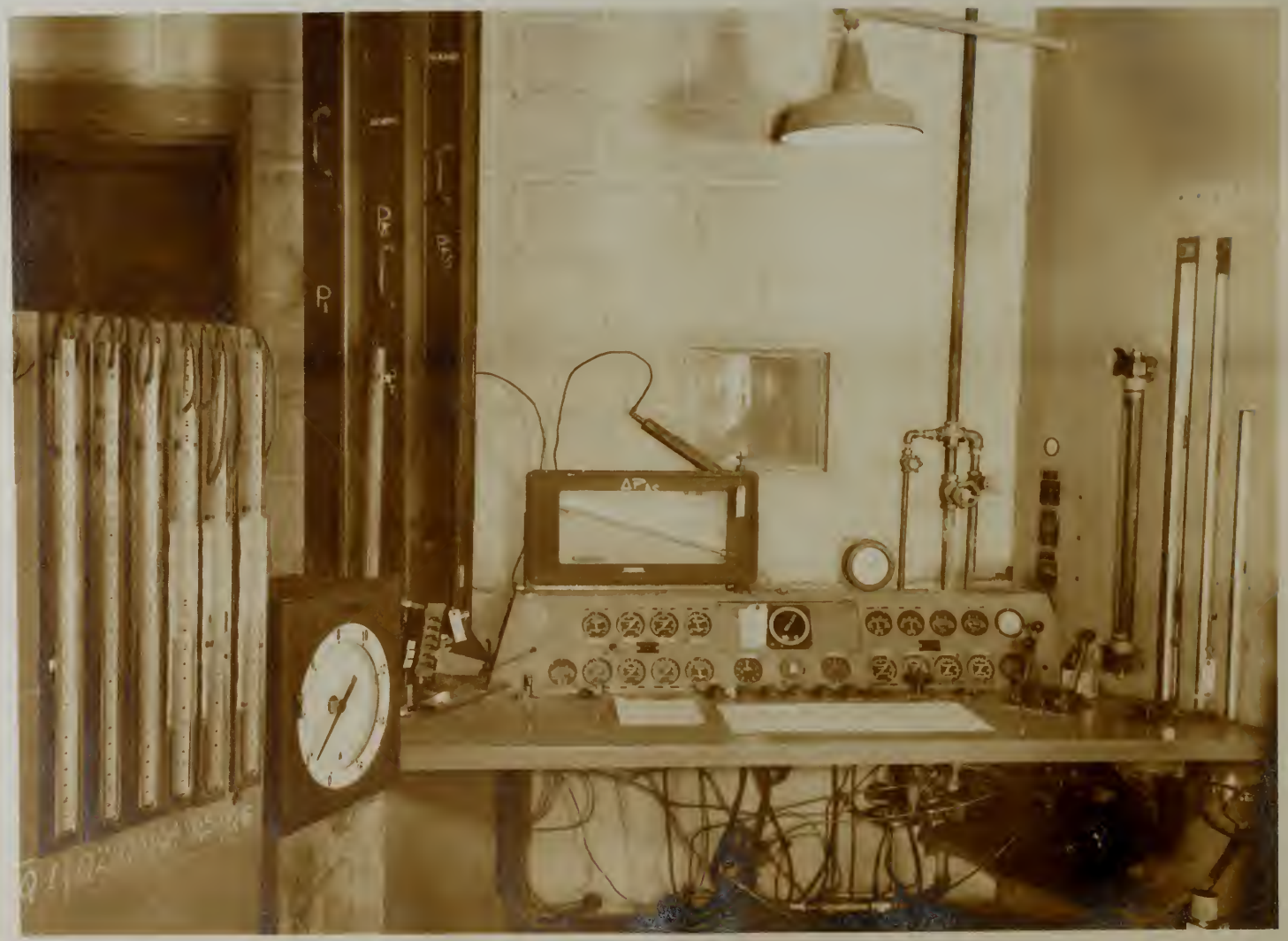

FIGURE 6

FIGURE 7

J-33 ENGINE DATA SCALED DOWN FOR SINGLE BURNER OPERATION

ALLISON DIVISION
GENERAL MOTORS CORP.

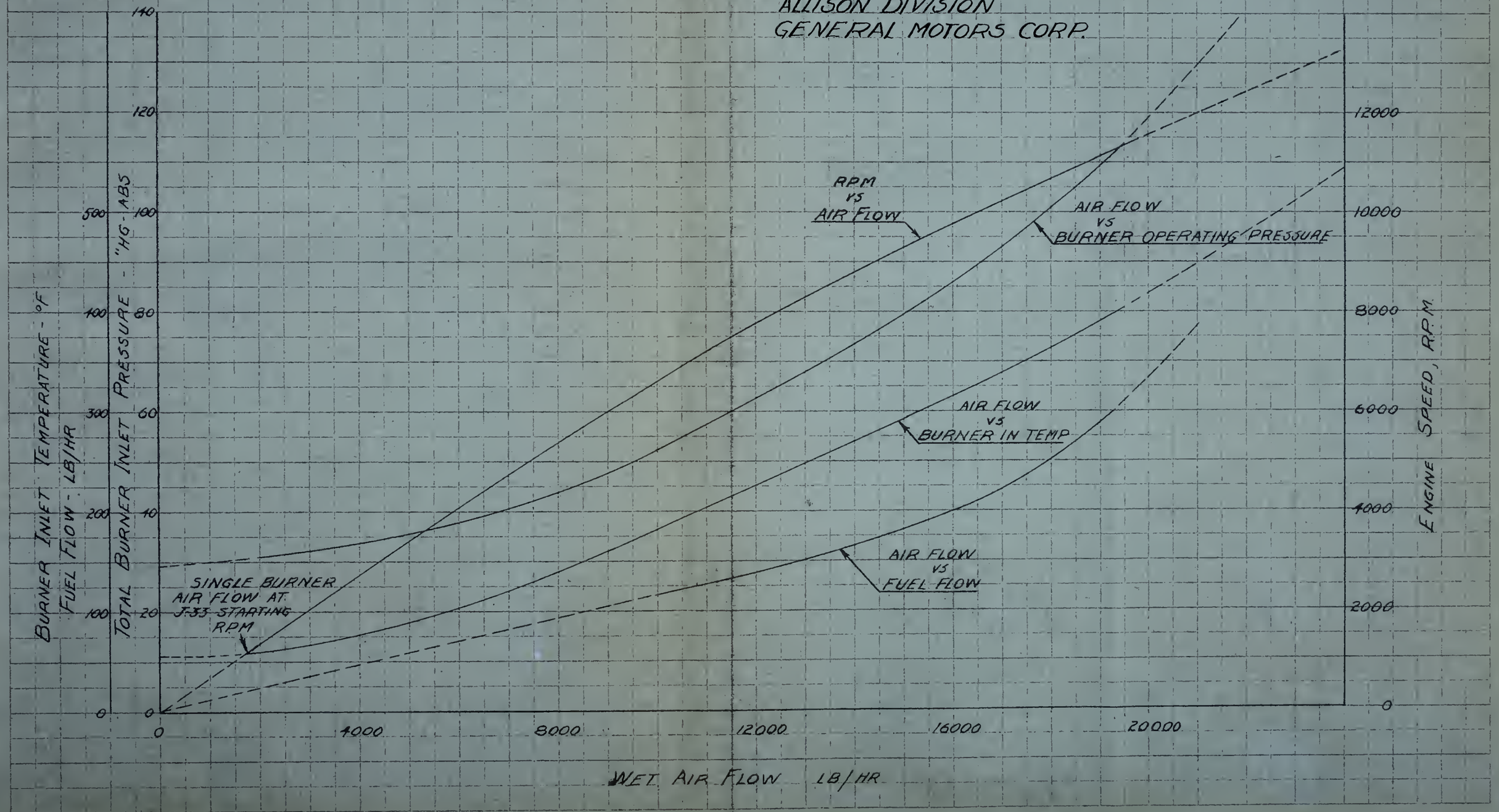

FIGURE 8

REPRESENTATIVE TEMPERATURE DISTRIBUTION ACROSS EXIT OF COMBUSTOR

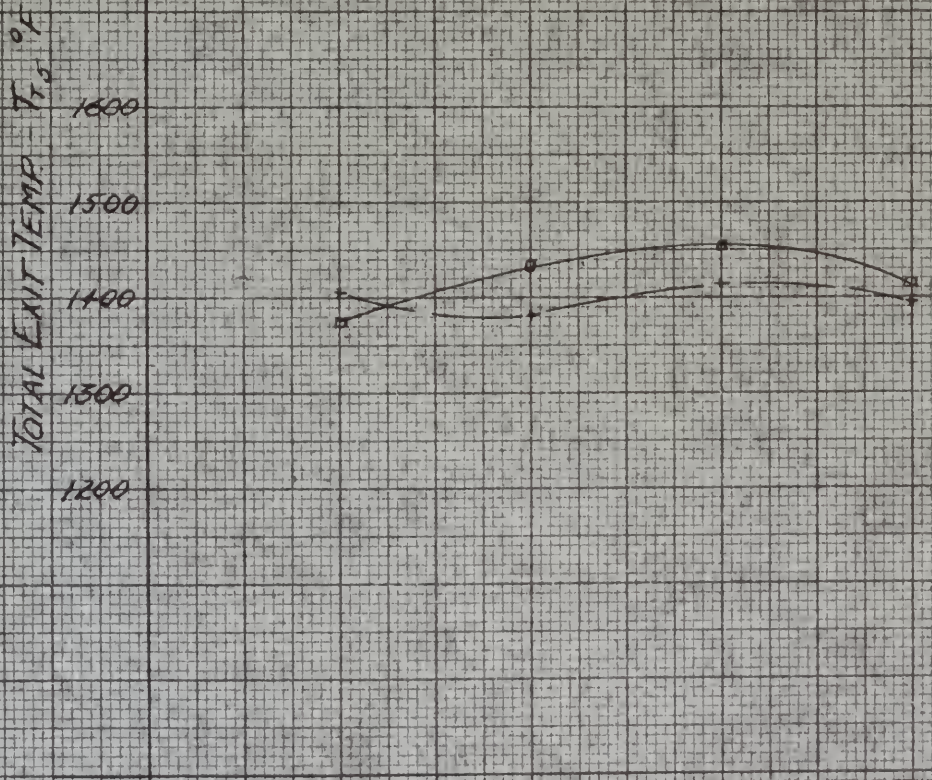

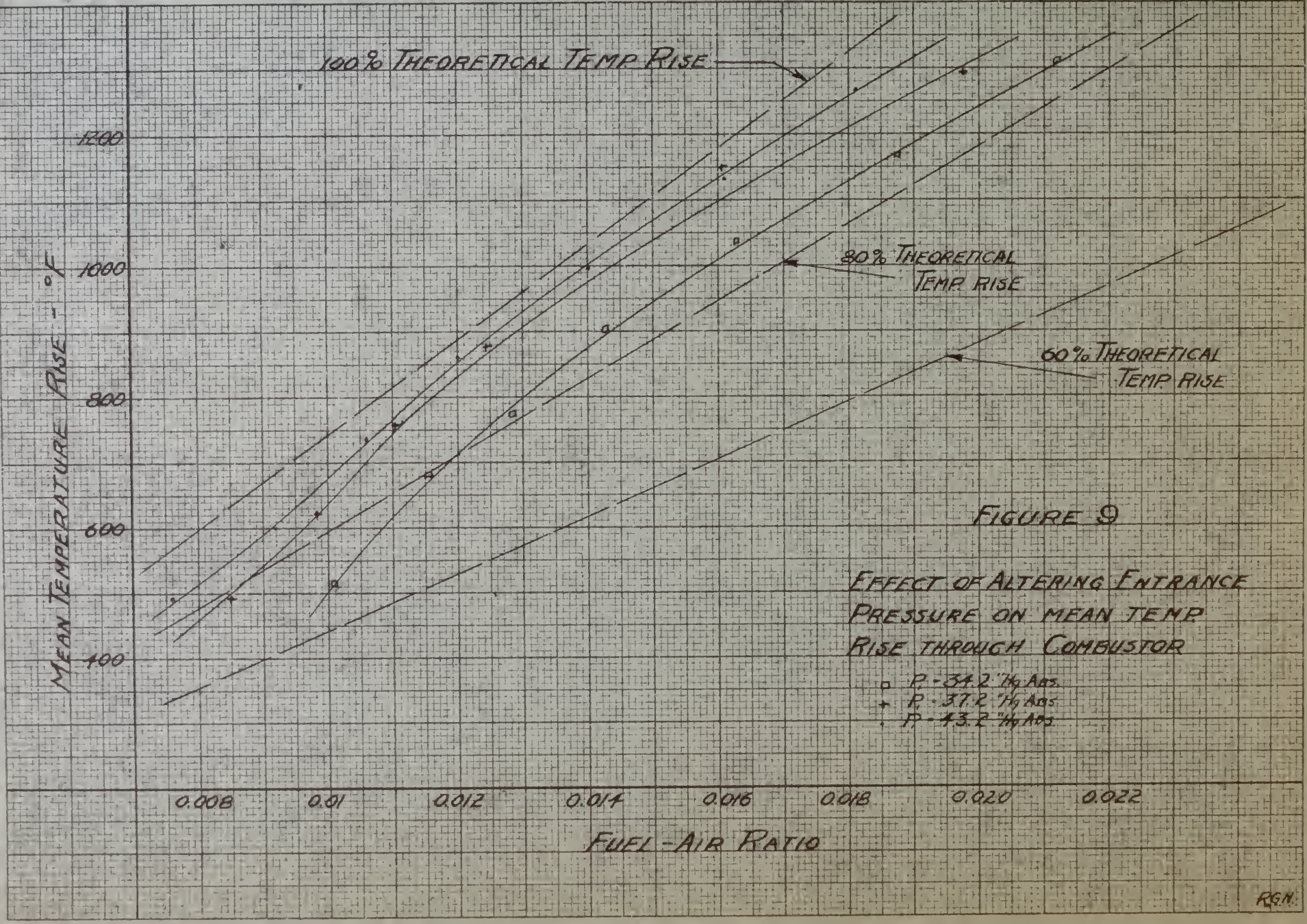

FIGURE 9

EFFECT OF ALTERING ENTRANCE PRESSURE ON MEAN TEMP RISE THROUGH COMBUSTOR

FIGURE 10

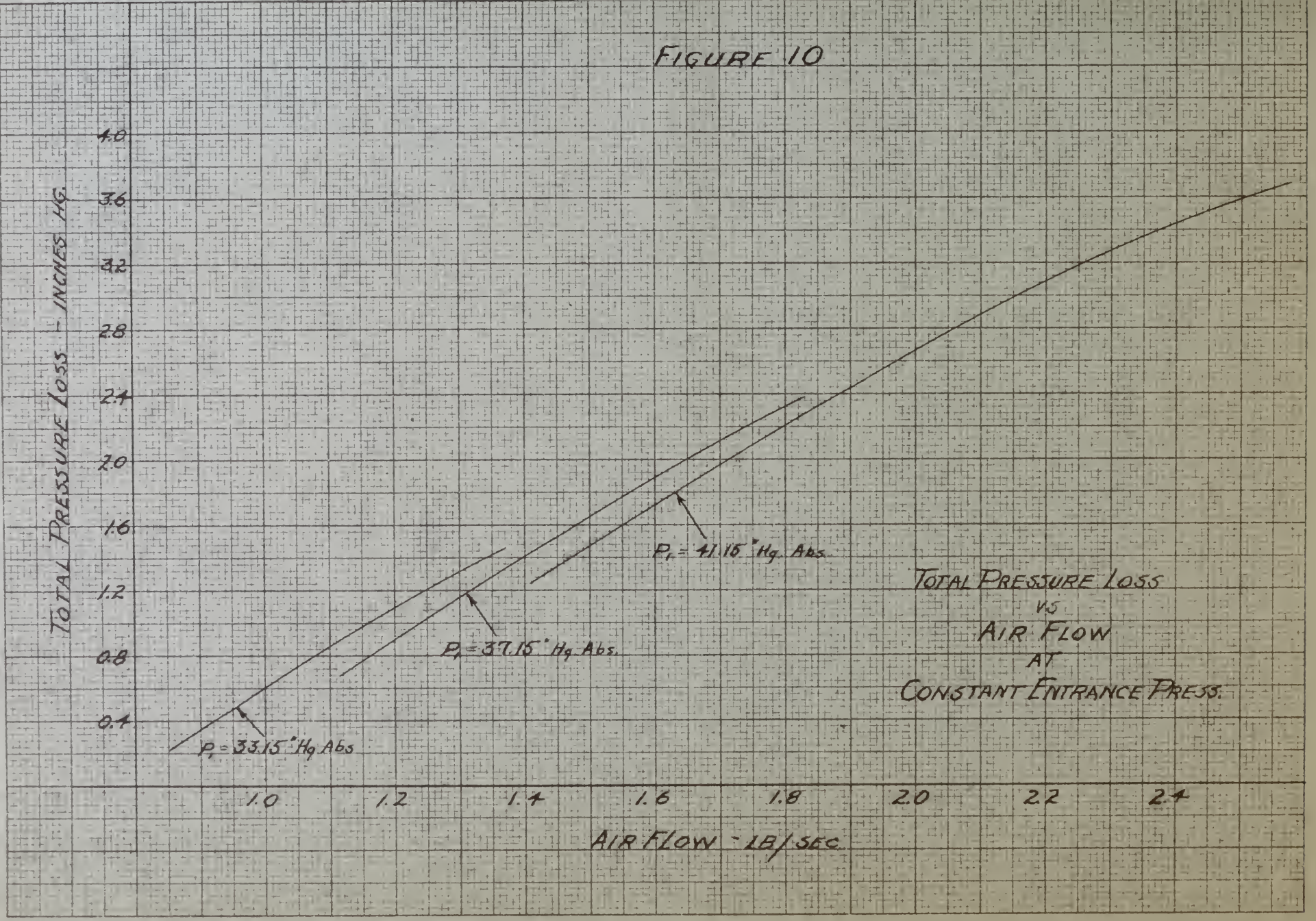
TOTAL PRESSURE LOSS - INCHES HG.
4.0
3.6
3.2
2.8
2.4
2.0
1.6
1.2
0.8
0.4
P_1 = 33.15 "Hg Abs
P_1 = 37.15 "Hg Abs.
P_1 = 41.15 "Hg. Abs.
TOTAL PRESSURE LOSS
VS
AIR FLOW
AT
CONSTANT ENTRANCE PRESS.
1.0
1.2
1.4
1.6
1.8
2.0
2.2
2.4
AIR FLOW - LB/SEC.

FIGURE 11

TOTAL PRESSURE LOSS
VS
AIR FLOW

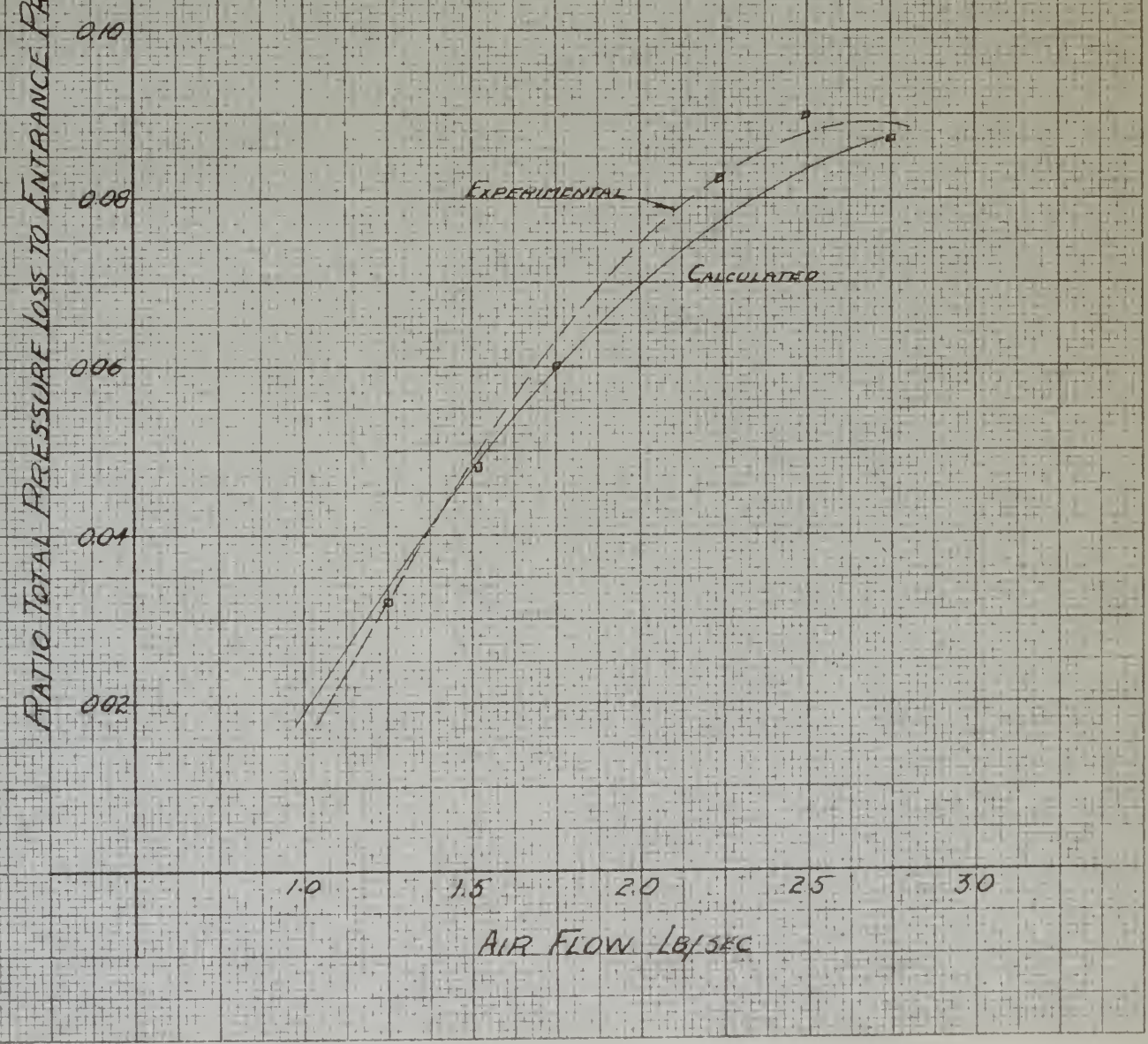

FIGURE 12

FRICTION PRESSURE LOSS VS AIR FLOW

□ EXPERIMENTAL DATA
+ CALCULATED - METHOD I
· CALCULATED - METHOD II

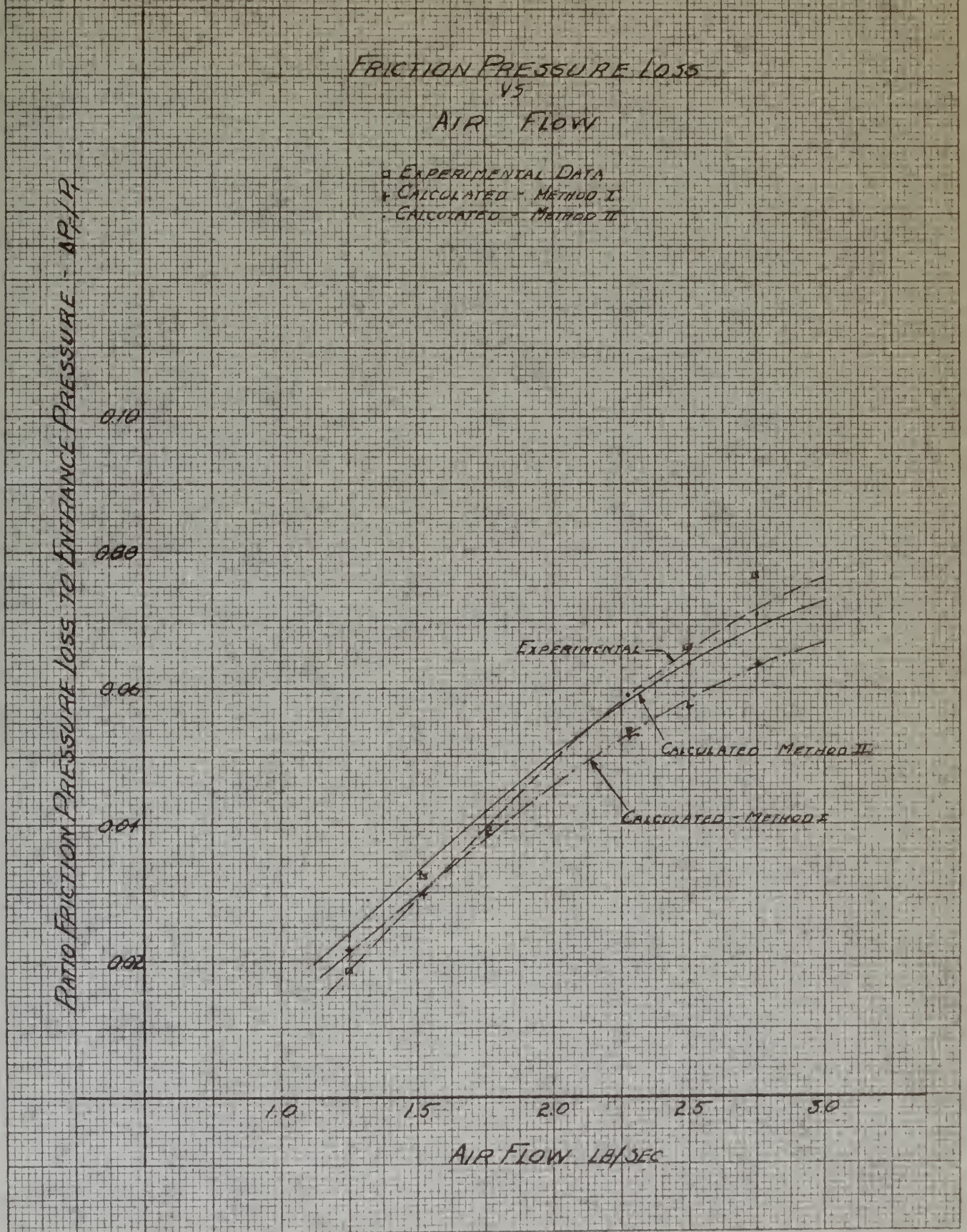

FIGURE 13

MOMENTUM PRESSURE LOSS
VS.
AIR FLOW

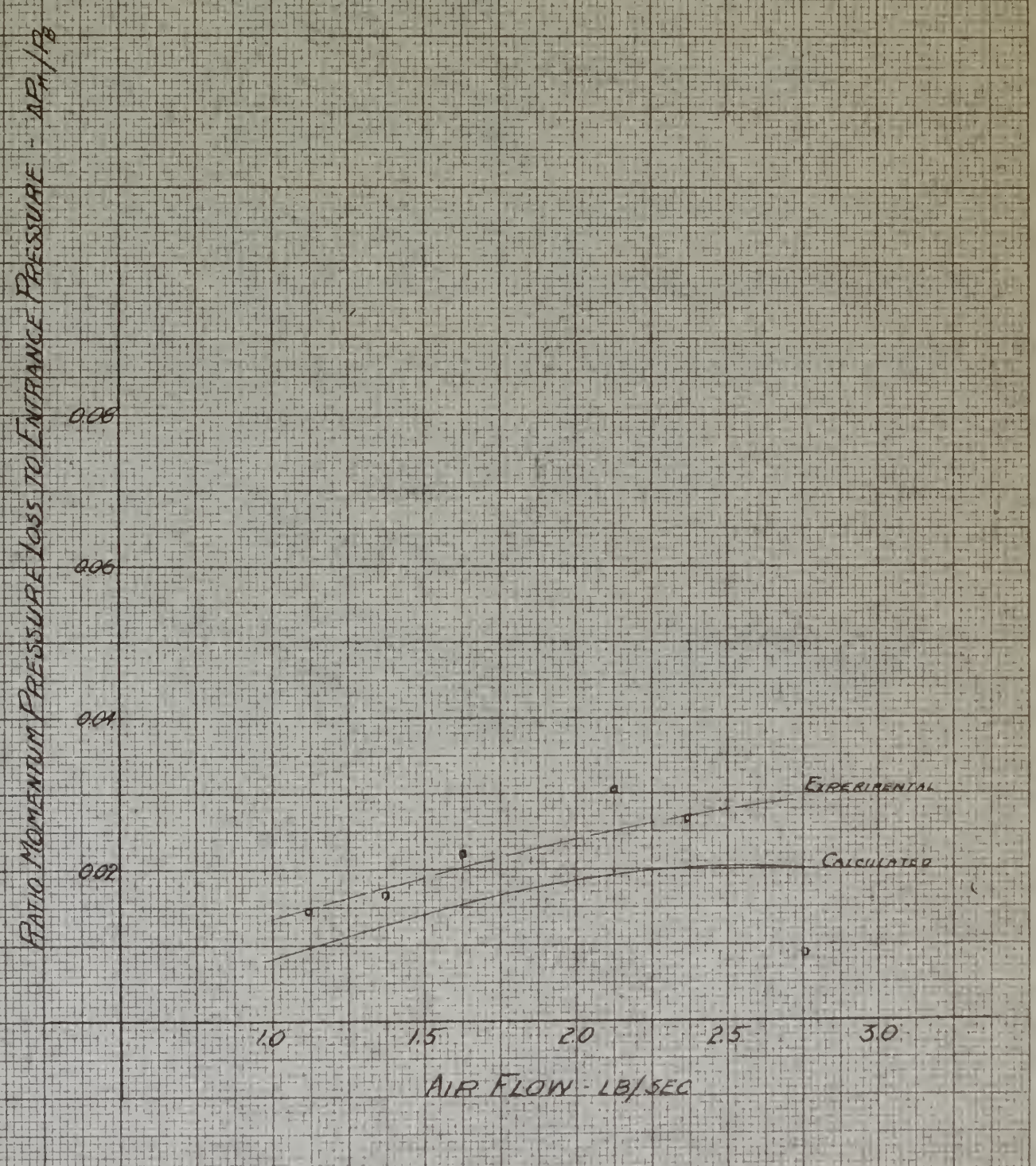

BIBLIOGRAPHY

1. GAS TURBINES FOR AIRCRAFT
   P. W. Godsey, Jr. and L. A. Young
   First Edition 1949
   McGraw-Hill Book Company, Inc.

2. GAS TURBINES AND JET PROPULSION FOR AIRCRAFT
   G. G. Smith, M. E. E.
   Fourth Edition 1946
   Aircraft Books, Inc.

3. EFFECT OF COMBUSTOR-INLET CONDITIONS ON PERFORMANCE OF AN ANNULAR TURBOJET COMBUSTOR
   N.A.C.A. T.N. NO. 1357
   J. H. Childs, R. J. McCafferty, and C. W. Burins.
   1947.

4. ANALYSIS OF JET PROPULSION ENGINE COMBUSTION CHAMBER PRESSURE LOSSES
   N.A.C.A. T.N. NO. 1180
   I. I. Pinkel and S Shaevs 1947

5. HANDBOOK OF ENGINEERING FUNDAMENTALS
   Eshbach
   First Edition
   John Wiley and Sons, Inc.

6. JET PROPULSION
   A Reference Text Prepared by the Staffs of the Guggenheim Aeronautical Laboratory and the Jet Propulsion Laboratory of Caleit, California Institute of Technology.
   C. S. Milliken and F. J. Malina.

BIBLIOGRAPHY

1. [illegible]
   [illegible]
   [illegible]
   [illegible]

2. [illegible]
   [illegible]
   [illegible]
   [illegible]

3. [illegible]
   [illegible]
   [illegible]
   [illegible]

4. [illegible]
   [illegible]
   [illegible]
   [illegible]

5. [illegible]
   [illegible]
   [illegible]
   [illegible]

6. [illegible]
   [illegible]
   [illegible]
   [illegible]
   [illegible]
   [illegible]
   [illegible]
   [illegible]

APPENDIX

Appendix - Analysis of Momentum Pressure Drop through Combustor

$$P_{T_1}/P_1 = (T_{T_1}/T_1)^{\gamma/\gamma-1}$$

$$P_{T_5}/P_5 = (T_{T_5}/T_5)^{\gamma/\gamma-1}$$

$$P_{T_5}/P_{T_1} = P_5/P_1 \,(T_{T_5}/T_{T_1})^{\gamma/\gamma-1}(T_1/T_5)^{\gamma/\gamma-1}$$

$$P = \rho RT$$

$$RT = PQ/w$$

$$P_1Q_1/T_1 = Rw = P_5Q_5/T_5$$

$$P_1V_1/T_1 = P_5V_5/T_5$$

$$P_{T_5}/P_{T_1} = V_1/V_5\; T_5/T_1\; (T_{T_5}/T_{T_1})^{\gamma/\gamma-1}(T_1/T_5)^{1/\gamma-1}$$

$$= V_1/V_5\,(T_{T_5}/T_{T_1})^{\gamma/\gamma-1}(T_1/T_5)^{1/\gamma-1}$$

$$P_{T_5} = P_{T_1}\, V_1/V_5\,(T_{T_5}/T_{T_1})^{\gamma/\gamma-1} \Big/ (T_5/T_1)^{1/\gamma-1}$$

To find T_1 & T_2

$$T_{T_1} = T_1\left(1 + \frac{\gamma-1}{2}M_1^2\right)$$

$$M_1^2 = V^2/a^2 = V_1^2/\gamma g R T_1$$

$$T_{T_1} = T_1\left[1 + \frac{\gamma-1}{2}(V_1^2/\gamma g R T_1)\right]$$

$$= T_1 + \frac{\gamma-1}{2}V_1^2/\gamma g R$$

$$= T_1 + V_1^2/2gR(\gamma/\gamma-1)$$

$$T_1 = T_{T_1} - V_1^2/2gR(\gamma/\gamma-1)$$

$$T_5 = T_{T_5} - V_5^2/2gR(\gamma/\gamma-1)$$

TO FIND V_5

$$P_1 A - P_5 A = \omega/g\,(V_5 - V_1)$$

$$P_1 Q/V_1 - P_5 Q_5/V_5 = \omega/g\,(V_5 - V_1)$$

$$PQ = RT\rho\frac{\omega}{g} = RT\omega$$

$$RT_1\omega/V_1 - PT_5\omega/V_5 = \omega/g\,(V_5 - V_1)$$

$$T_1/V_1 - T_5/V_5 = (V_5 - V_1)/Rg$$

DIVIDING (2) & (3) by V_1 & V_5

$$T_1/V_1 = T_{T_1}/V_1 - V_1/2gR(\gamma/\gamma-1)$$

$$T_5/V_5 = T_{T_5}/V_5 - V_5/2gR(\gamma/\gamma-1)$$

$$T_1/V_1 - T_5/V_5 = T_{T_1}/V_1 - T_{T_5}/V_5 + (V_5 - V_1)/2gR(\gamma/\gamma-1)$$

$$T_{T_1}/V_1 - T_{T_5}/V_5 + (V_5 - V_1)/2gR(\gamma/\gamma-1) = 1/Rg\,(V_5 - V_1)$$

$$T_{T_1}/V_1 - T_{T_5}/V_5 = 1/Rg\,(V_5 - V_1) - (V_5 - V_1)/2gR(\gamma/\gamma-1)$$

$$= (V_5 - V_1)\left(\frac{1}{Rg} - 1/2gR(\gamma/\gamma-1)\right)$$

$$= (V_5 - V_1)\left(\frac{2\gamma - (\gamma-1)}{2gR\gamma}\right)$$

$$= (V_5 - V_1)\left(\gamma+1/2\gamma gR\right)$$

$$T_{T_1}/V_1\left[1 - \frac{T_{T_5}/V_5}{T_{T_1}/V_1}\right] = \left(\frac{\gamma+1}{2gR}\right)V_1\left(V_5/V_1 - 1\right)$$

$$T_{T_1}/V_1\left[1 - \frac{T_{T_5}}{T_{T_1}}\,\frac{V_1}{V_5}\right] =$$

$$1 - \frac{T_{T_5}}{T_{T_1}}\frac{V_1}{V_5} = \frac{\gamma+1}{2}\left(M_{1_T}^2\right)\left(\frac{V_5}{V_1} - 1\right)$$

$$1 - \frac{T_{T_5}/T_{T_1}}{V_5/V_1} = \frac{\gamma+1}{2}\left(M_{1_T}^2\right)\frac{V_5}{V_1} - \frac{\gamma+1}{2}M_{1_T}^2$$

$$1 + \frac{\gamma+1}{2}M_{1_T}^2 = \frac{\gamma+1}{2}M_{1_T}^2\frac{V_5}{V_1} + \frac{T_{T_5}}{T_{T_1}}\Big/\frac{V_5}{V_1}$$

$$\left(V_5/V_1\right)^2\frac{\gamma+1}{2}M_{1_T}^2 - V_5/V_1\left[1 + \frac{\gamma+1}{2}M_{1_T}^2\right] + T_{T_5}/T_{T_1} = 0$$

$$V_5/V_1 = 1 + \frac{\gamma+1}{2}M_{1_T}^2 \pm \sqrt{\left(1 + \frac{\gamma+1}{2}M_{1_T}^2\right) - 4\left(\frac{\gamma+1}{2}M_{1_T}^2\right)T_{T_5}/T_{T_1}}\Big/(\gamma+1)M_{1_T}^2$$

Analysis of Friction Pressure Drop Through the Combustion Chamber

Flow through an Orifice

$$\Delta P_F = \rho/2g \left[\frac{Q}{\rho} \frac{\sqrt{1-\left(\frac{A_2}{A_1}\right)^2}}{A_2 C} \right]^2$$

A_1 = Area in Annular Space, square feet

A_2 = Orifice Area, square feet

C = Orifice Coefficient

ΔP = Pressure Drop Across Orifice, lb/sq.ft.

ρ = Density of Fluid, lb/ft^3

Q = Mass Flow through Orifice, cu.ft./sec

Assume Parallel Flow System. Pressure Drop Across One Orifice Equal Pressure Drop Across Any Orifice. Check For Constant Mass Flow.

SYMBOLS

The symbols used in this paper are those being currently used for turbo-jet engines.

A	Area of any cross section, square feet
M	Mach number, ratio of airspeed to local speed of sound
P_T	Total pressure, pounds per square foot or inches of mercury
P	Static pressure, pounds per square foot or inches of mercury
ΔP_T	Total pressure loss due to friction and heat addition, inches of mercury
ΔP_F	Friction pressure loss, inches of mercury
ΔP_M	Momentum pressure loss, inches of mercury
T_T	Total temperature, degrees Rankine
T	Static temperature, degrees Rankine
V	Velocity of gas flow, feet per second
W	Air mass flow, pounds per second
Q	Air mass flow, cubic feet per second
γ	Ratio of specific heat at constant pressure to specific heat at constant volume
ρ	Density of air, pounds per cubic foot

Subscripts

1	Combustor inlet
5	Combustor outlet
E	Equivalent combustor or constant cross-sectional area

Glossary

The glossary words in this lesson and those having more-
mostly about the three-letter endings.

A	Name of any human habitat, object that
B	Used mainly, refers to substance in their stead of human
B^2	Their pronoun, denotes the objects that do instead of
	mankind
C	Mainly pronoun, covers the objects that do instead of
	mankind
D^2	Their possessive pronoun that is similar and their modifier,
	Items of ownership
D^3	Material possessive noun, refers to ownership
D^4	Something possessive noun, refers to ownership
E^2	Their conjunction, relates qualities
I	Mainly pronoun, refers to human position
A	Definitely of time, like our moment
E	Air mass flow, denotes hot country
G	Air mass flow, mainly cool but moving
H^2	Verb of physical type of movement, relates to physical
	ways of physical things
L	Mainly of air, usually our body line
	movements
I	Conjugator verb
S	Conjugator verb
T^2	Conjugator verb
	(Different conjugator or connecting word-modifier) word

GLOSSARY

The glossary words in this chapter are those terms commonly used for turbo-jet engines.

A Area of any given condition, square feet

B Bleed manifold, units of airplane to local source of pressurized

B_T^2 Total pressure, pounds per square foot or inches of mercury

I Static pressure, pounds per square foot or inches of mercury

ΔT_T^2 Total pressure loss due to friction and heat addition, inches of mercury

ΔT_S^2 Friction pressure loss, inches of mercury

ΔP_S^2 Compressor pressure rise, inches of mercury

T_T^2 Total temperature, degrees Rankine

T Static temperature, degrees Rankine

V Velocity or gas flow, feet per second

W Air mass flow, pounds per second

W_f Air mass flow, units that are metered

$\frac{W\sqrt{\theta}}{\delta}$ Ratio of corrected mass air flow to corrected compressor air pressure ratio

η_c Velocity of air, decimal part ratio flow

Subscripts

1 Compressor inlet

2 Compressor outlet

3 Diffusion section or combustion chamber-turbine area

DATE DUE			
21 FE'50			

Thesis 11471
N42 Nester
Testing a turbo-jet
combustion chamber to
check analytical design.

Thesis 11471
N42 Nester
Testing a turbo-jet
combustion chamber to
check analytical design.

thesN42
Testing a turbo-jet combustion chamber t
3 2768 001 89912 3
DUDLEY KNOX LIBRARY